Investigation on a thermal-coupled two-stage pulse tube cryocooler with multi-bypass working at 8 K

Mingtao Pan[1,2,3],Bin Yang[1,2,3],Nailiang Wang[1,2],Enchun Xing[1,2,3], Bo Tian[1,2,3], Chenglong Liu[1,2,3],Yanen Li[1,2,3] , Jia Quan[1,2*], Miguang Zhao[1,2]

[1]Technical Institute of Physics and Chemistry,Chinese Academy of Science, Beijing, China
[2]State Key Laboratory of Cryogenic Science and Technology, Technical Institute of Physics and Chemistry, Chinese Academy of Science, Beijing, China
[3]University of Chinese Academy of Sciences, Beijing, China

[*]E-mail: quanjia10@mail.ipc.ac.cn

Abstract. The Stirling type pulse tube cryocooler (SPTC) eliminates moving parts at the cold end and is driven by a linear compressor at the hot end, thus offering the advantages of low vibration at both ends, high reliability, and long service life, which makes it attractive for various special fields, such as the space field.In practice, there is an increasing interest in providing cooling power at different temperature levels. This paper presents an experimental investigation of a thermal-coupled two-stage pulse tube cryocooler with multi-bypass structures. The experiments investigated the effects of the second-stage operating frequency, charging pressure, and input power on performance. Building upon this, the study explored the interaction between the first-stage temperature, multi-bypass temperature, and second-stage temperature, alongside experimental testing of cooling performance. The experimental results show that through the thermal coupling pre-cooling and the design of multi-bypass structure, the second-stage cold finger can realize the lowest temperature of 5.2 K and the cryocooler can provide 54 mW cooling capacity at 8 K while providing 50 mW cooling capacity at 35 K with the 1st-stage providing 1.5 W of cooling capacity.

1.Introduction

As important wireless electronic components, terahertz detectors are widely used in many fields such as communication, imaging, and astronomical observation[1,2]. Meanwhile, the pulse tube cryocooler has become a key device for realizing the low-temperature operating environment of terahertz detectors[2–4]. The core components of the indium antimonide hot electron bolometers need to operate at temperatures below 10 K. Single-stage pulse-tube cryocoolers are primarily focused on applications in the 80 K[5,6], 60 K[7], and 40 K[8–10] temperature ranges. Currently, they cannot achieve operation in the 8 K temperature range, leading to increasing research efforts directed toward two-stage pulse-tube cryocoolers[11–16]. Most existing studies on two-stage PTCs focus on providing cooling in the liquid hydrogen temperature region[13,15], it remains challenging to reach temperatures below 10 K. For example, Yang et.al (2008) developed a thermally-coupled two stage pulse tube cooler with double inlet orifice as the phase shifter and a no load temperature of 12.8 K was obtained[17]; Qiu et al. (2012) reported a two-stage thermally coupled with pre-cooling pulse tube type cryocooler, which achieved a no-load

temperature of 15.87 K[18]; Pang et al. (2017) designed and optimized a thermally-coupled two-stage pulse tube with a target of cooling power 1.0 W at 10 K[19]; Wu et al. (2021) developed a two-stage PTC with Er-plated screens as regenerator material, achieving a minimum temperature of 14.95 K at the second stage[12]; Even fewer studies have reported two-stage PTCs capable of reaching temperatures below 8 K, which is critical for high-performance THz detectors[2].

Yang et al. (2025) recently proposed a thermal-coupled two-stage high-frequency PTC with hybrid Er_3Ni/stainless steel screen regenerative material, achieving a minimum second-stage temperature of 9.1 K[11]. While this represented progress, it still fell short of the sub-8 K requirement for advanced InSb-based THz detectors. To address this, we experimentally investigate a thermally-coupled two-stage pulse tube cryocooler with a multi-bypass structure for 8 K operation. The study optimizes second-stage parameters, examines interstage thermal interactions, and evaluates simultaneous cooling performance at multiple temperatures, demonstrating the potential of this PTC to meet the cryogenic demands of THz detectors.

2. Experimental Apparatus

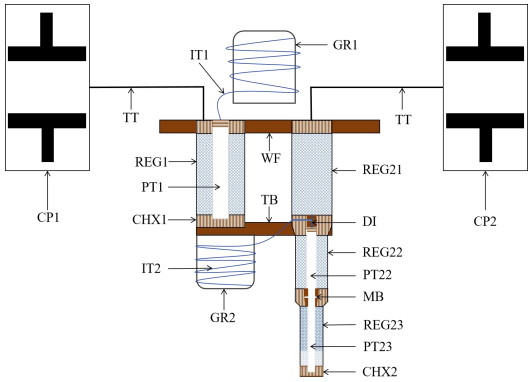

CP1:compressor of 1st-stage; CP2:compressor of 2nd-stage; TT:transfer tube; REG1:1st-stage regenerator; PT1:1st-stage pulse tube; CHX1:1st-stage cold end heat exchanger; IT1:1st-stage inertance tube; GR1:1st-stage gas reservoir; GR2:2nd-stage gas reservoir;REG21:pre-regenerator; REG22:2nd-stage regenerator(first section); PT22:2nd-stage pulse tube(first section); REG23:2nd-stage regenerator(second section); PT23:2nd-stage pulse tube(second section); CHX2:2nd-stage cold end heat exchanger; MB:Multi-Bypass; DI:double-inlet; WF:hot end flange; TB:thermal bridge.

Figure 1.Schematic diagram of two-stage thermal-coupled cold finger structure with multi-bypass.

Figure 1 shows a schematic diagram of a two-stage thermal-coupled cold finger structure with a multi-bypass. The cold finger is driven by two proprietary dual-piston opposed compressors (Model: first stage is CP300, second stage is THz500). The first stage pre-cools the second stage via thermal bridges, with both stages using a coaxial layout for compactness. Phase shifters comprise room-temperature components (inertance tube + 400 cc reservoir) for the first stage and cold components (inertance tube + 230 cc reservoir, mounted on the bridge) for the second. A multi-bypass assembly provides additional phase adjustment on the second stage.

A copper water cooling disk is attached to the flange at the room temperature end to provide 10 ℃ cooling water through a water chiller, and the compressor is cooled using air

cooling. A photograph of the two-stage thermal-coupled cold finger with multi-bypass is shown in Figure 2. To isolate external radiative heat transfer, the cold finger is wrapped in approximately 15 layers of aluminum foil (as shown in Figure 2). This assembly is then housed within a vacuum chamber (maintained below 10^{-5}Pa) to minimize convective heat transfer, ensuring efficient cooling.

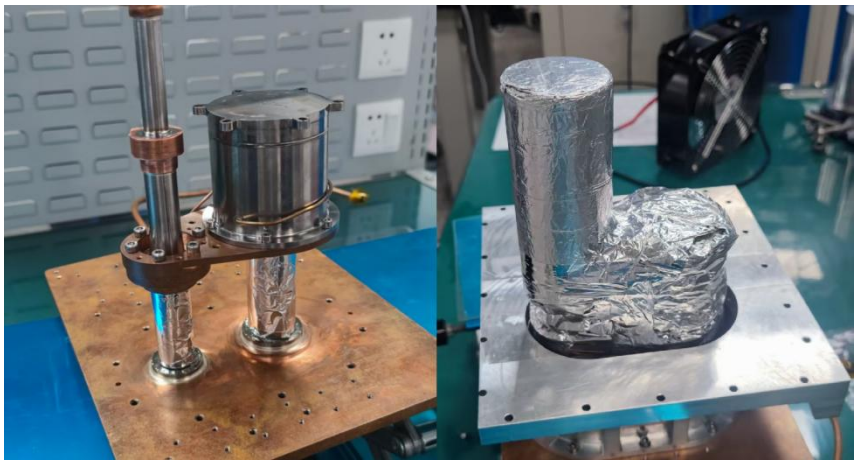

Figure 2. A photograph of the two-stage thermal-coupled cold finger with multi-bypass.

The regenerator REG23 is filled with a mixture of $HoCu_2$ particles and Er_3Ni particles, and the rest of the regenerator are filled with stainless steel screen (SSS) of different mesh sizes. The filling method and filling material parameters for the REG23 are shown in Table 1.

Table 1. REG23 filling method and filling material parameters.

Regenerator	Regenerator filling method	Material parameters
REG23	25%#250-300 $HoCu_2$+25%#200-250 Er_3Ni+50%#150-200 Er_3Ni	Sphere diameter (μm): #250-300 $HoCu_2$:55 #200-250 Er_3Ni:75 #150-200 Er_3Ni:154

3. Experimental results and analysis

Experiments focused on optimizing the second-stage performance by varying its operating frequency, charging pressure, and input power. Interactions among the first-stage, bypass, and second-stage temperatures were also examined, followed by an evaluation of simultaneous cooling capability at multiple temperature zones. Based on prior optimization, the first-stage operating frequency and charging pressure were fixed at 42 Hz and 4.0 MPa, respectively.

3.1 Influence of 2nd-stage operating frequency on cooling performance

The cooling performance of the second stage improved with decreasing operating frequency, as shown in Figure 3. Reducing the frequency from 20 Hz to 16 Hz increased the cooling capacity at 8 K from 37 mW to 62 mW. The lowest feasible frequency was 15.5 Hz due to power supply limitations; thus, 16 Hz was selected as the optimal operating frequency. This

trend is attributed to the improved thermodynamic efficiency at lower frequencies. A slower cycle enhances heat transfer within the regenerator and allows the inertance tube to more effectively shift the phase between the pressure wave and the mass flow, which is critical for performance at cryogenic temperatures.

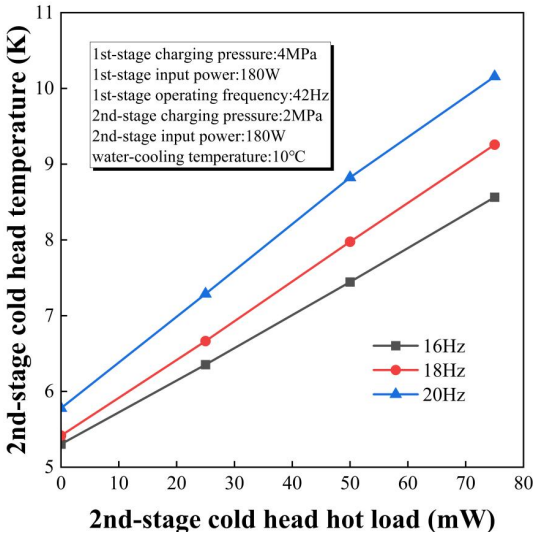

Figure 3. Influence of 2nd-stage operating frequency on cooling performance.

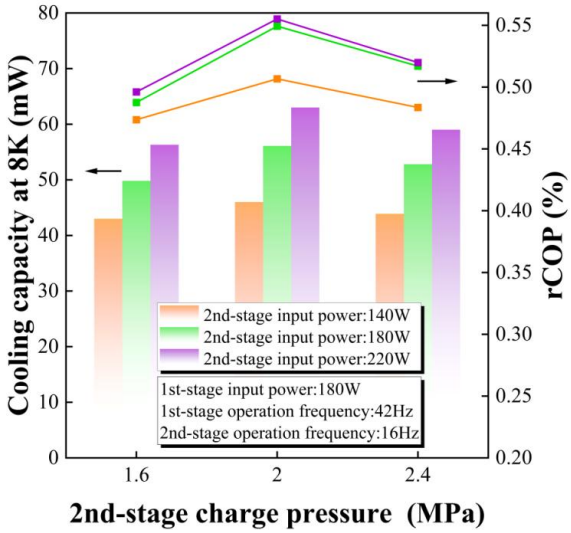

Figure 4. Influence of 2nd-stage charging pressure and input power on cooling performance.

3.2 Influence of 2nd-stage charging pressure and input power on cooling performance

The cooling performance of the second stage under different charging pressures and input powers is shown in Figure 4. The cooling capacity at 8 K increases with higher input power due to enhanced enthalpy flow. However, increasing the charging pressure beyond 2.0 MPa reduces

cooling performance due to increased regenerator pressure losses. Optimal performance was achieved at 2.0 MPa charging pressure with 220 W input power. This non-monotonic behavior results from a competition between two effects: higher pressure increases the gas density and thus the cooling power, but it also leads to disproportionately larger pressure drop losses in the regenerator. The optimum pressure represents the balance point where the net cooling power is maximized.

3.3 Interaction between 1st-stage, multi-bypass and 2nd-stage temperatures

In order to investigate the interaction law of interstage temperatures, an experimental study was conducted to investigate the interaction between the 1st-stage temperature, multi-bypass temperature and the 2nd-stage temperature. (Note: Results are specific to the compressor model used. Performance may vary with other compressors due to differing phase and impedance characteristics. All temperature data represent steady-state averages, recorded when fluctuations remained within ±0.1 K (2nd stage) and ±0.5 K (1st stage and bypass) for 30 minutes. Data points were collected at 5-minute intervals and averaged.)

Figure 5 shows the effect of the first-stage temperature on the multi-bypass and second-stage temperatures. The first-stage temperature was varied by adjusting a heater attached to its cold head. Both the multi-bypass and second-stage temperatures showed low sensitivity to changes in the first-stage temperature, with rates of change of approximately 0.08 K/K and 0.015 K/K, respectively, indicating that fluctuations in the first-stage temperature have minimal impact.

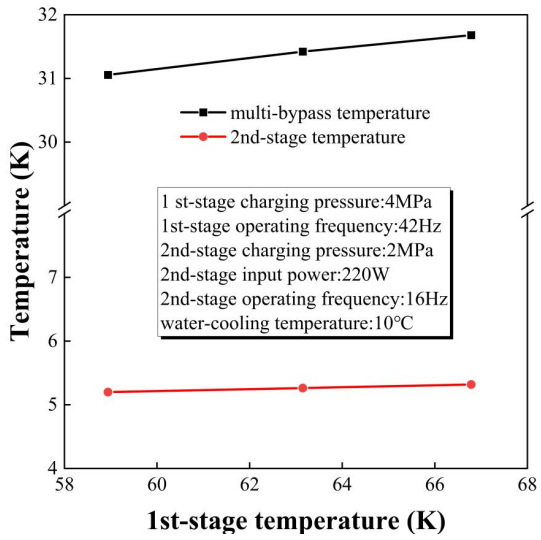

Figure 5. Effect of the 1st-stage temperature on the multi-bypass temperature and the 2nd-stage temperature.

As shown in Figure 6, temperature variations at the multi-bypass had limited influence on both the first and second stage temperatures. The temperature sensitivity coefficients were measured at 0.08 K/K for the first stage and 0.047 K/K for the second stage, demonstrating minimal thermal interaction between the multi-bypass and the main cooling stages.

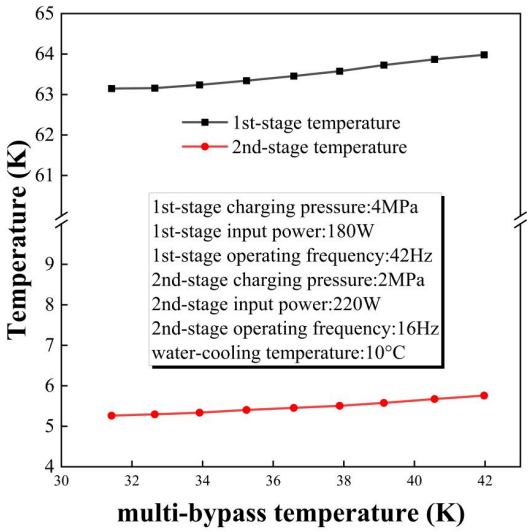

Figure 6. Effect of the multi-bypass temperature on the 1st-stage temperature and the 2nd-stage

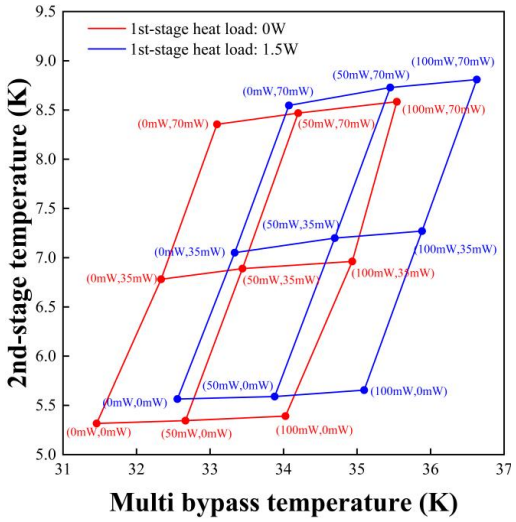

Figure 7. Cooling performance for providing cooling at different temperatures simultaneously.

3.4 Cooling performance that provides cooling at different temperatures simultaneously

The second-stage cold head cools electronic chips, while the multi-bypass cools connecting wires to minimize heat transfer from warmer regions. The first-stage heating load simulates cold screen heat leakage.

Figure 7 shows the cooling performance for providing cooling at different temperatures simultaneously. To ensure thermal balance and data reliability, temperature and power data for each load point are recorded only after the temperature has stabilized and remained constant for 2 hours. The system was tested with and without first-stage heating loads. Applied heat loads affected multi-bypass and second-stage performance through thermal coupling. After

optimization, the cryocooler simultaneously provided 54 mW at 8 K, 50 mW at 35 K, and 1.5 W at the first stage.

3.5 Measurement uncertainty

The uncertainties of the measured parameters are based on the accuracies of the instruments listed in Table 2. The combined standard uncertainty for the cooling capacity measurements is estimated to be within ±5%.

Table 2. Key measurement instruments and their accuracy.

Measuring device	Device model	Accuracy
AC Power Supply	DH18614	±(1% of reading + 3 digits)
Digital Power Meter	EVERFINE PF2010	±(0.04% of reading + 0.04% range)
DC Power Supply	MYWAVE 3303S	V: ±(0.03% + 10 mV); I: ±(0.3% + 10 mA)
Data Acquisition Instrument	Keithley 2700	±(0.005% of reading + 0.015 K)
Temperature Sensor (General)	PT100	±(0.15% of reading + 0.03 K)
Temperature Sensor (2nd-Stage)	DT670 Diode	±12 mK @ 2.5-20 K

4. Conclusions

An experimental study was conducted on a two-stage thermally-coupled pulse tube cryocooler with multi-bypass. Optimal performance was achieved at second-stage conditions of 2.0 MPa charging pressure, 16 Hz operating frequency, and 220 W input power. Thermal interactions between stages showed minimal sensitivity, with first-stage variations having negligible impact on multi-bypass and second-stage temperatures. The system demonstrated simultaneous cooling capacity of 54 mW at 8 K, 50 mW at 35 K, and 1.5 W at the first stage, reaching a minimum temperature of 5.2 K at the second stage.

Acknowledgments

This work is supported by National Key R&D Program of China under grant：2023YFB3905600，2023YFB3905603.

References

[1] Clochiatti S, Grygoriev A, Kress R, et al. Low-Noise Resonant Tunneling Diode Terahertz Detector[J]. IEEE Transactions on Terahertz Science and Technology, 2025, 15(1): 107-119. https://ieeexplore.ieee.org/document/10766652/. doi: 10.1109/TTHZ.2024.3505599.

[2] Quan J, Liu Y, Liu D, et al. 4 K high frequency pulse tube cryocooler used for terahertz space application[J]. CHINESE SCIENCE BULLETIN, 2014, 59(27): 3490-3494. https://link.springer.com/article/10.1007/s11434-014-0457-5. doi: 10.1007/s11434-014-0457-5.

[3] Collaboration T N, Wex A, Rothe J, et al. Decoupling Pulse Tube Vibrations from a Dry Dilution Refrigerator at mi lli-Kelvin Temperatures[M]. arXiv, 2025. http://arxiv.org/abs/2501.04471. doi: 10.48550/arXiv.2501.04471.
[4] Zhang A, Han Y, Guo S, et al. Effect of reject temperature on aerospace pulse tube refrigerator[J]. Applied Therma l Engineering, 2023, 224: 120092. https://linkinghub.elsevier.com/retrieve/pii/S1359431123001217. doi: 10.1016/j.applthermaleng.2023.120092.
[5] Wang N, Tang Q, Xun Y, et al. A lightweight high-capacity pulse tube cryocooler operating at 80 K[J]. Cryogenics, 2024, 138: 103800. https://linkinghub.elsevier.com/retrieve/pii/S0011227524000201. doi: 10.1016/j.cryo genics.2024.103800.
[6] Tian B, Liu C, Tang Q, et al. A single coaxial pulse tube cryocooler with high specific mass operating at 80 K devel oped based on simulation and experimental methods[J]. Cryogenics, 2025, 149: 104104. https://linkinghub. elsevier.com/retrieve/pii/S0011227525000839. doi: 10.1016/j.cryogenics.2025.104104.
[7] Li Y, Wang N, Zhao M, et al. Numerical and experimental investigation of 12 W/60 K high-efficiency coaxial pulse tube cryocooler[J]. Cryogenics, 2024, 143: 103941. https://linkinghub.elsevier.com/retrieve/pii/S0011227 524001619. doi: 10.1016/j.cryogenics.2024.103941.
[8] Dang H. 40K single-stage coaxial pulse tube cryocoolers[J]. Cryogenics, 2012, 52(4-6): 216-220. https://linking hub.elsevier.com/retrieve/pii/S001122751200015X. doi: 10.1016/j.cryogenics.2012.01.014.
[9] Wang G, Cai J, Jing W, et al. Development of a 0.5 W/40 K Pulse Tube Cryocooler for an Infrared Detector[C]//Cr yocoolers 14. 2007.
[10] Zhang A, Wu Y, Liu S, et al. High-efficiency 3 W/40 K single-stage pulse tube cryocooler for space application[J]. Cryogenics, 2018, 90: 41-46. https://linkinghub.elsevier.com/retrieve/pii/S001122751730351X. doi: 10.10 16/j.cryogenics.2018.01.004.
[11] Yang B, Liu Z, Gao M, et al. Cooling performance improvement of a thermal-coupled two-stage high-frequency p ulse tube cryocooler with hybrid Er3Ni/stainless steel screen regenerative material[J]. Applied Thermal Eng ineering, 2025, 261: 125222. https://linkinghub.elsevier.com/retrieve/pii/S1359431124028904. doi: 10.10 16/j.applthermaleng.2024.125222.
[12] Wu W, Cui X, Liu S, et al. Cooling performance improvement of a two-stage pulse tube cryocooler with Er-plated screen as regenerator material[J]. International Journal of Refrigeration, 2021, 131: 615-622. https://linkin ghub.elsevier.com/retrieve/pii/S0140700721003376. doi: 10.1016/j.ijrefrig.2021.08.007.
[13] Li Z W, Wang X T, Wang Y N, et al. Development of a 20K two-stage Stirling type pulse tube cryocooler with pre-c ooling inside second-stage pulse tube[J]. IOP Conference Series: Materials Science and Engineering, 2022, 12 40(1): 012134. https://iopscience.iop.org/article/10.1088/1757-899X/1240/1/012134. doi: 10.1088/175 7-899X/1240/1/012134.
[14] Nguyen C. Hydrogen/Oxygen Propellant Densifier Using a Two-Stage Pulse Tube Cryocooler[C]//AIP Conferenc e Proceedings: Vol. 710. Anchorage, Alaska (USA): AIP, 2004: 1703-1712. https://pubs.aip.org/aip/acp/artic le/710/1/1703-1712/1000334. doi: 10.1063/1.1774869.
[15] Zhenhua J, Jiantang S, Shaoshuai L, et al. Influence of frequency and pressure on entropy production characterist ics of regenerator at 20 K pulse tube cryocooler[J]. International Journal of Refrigeration, 2022, 144: 222-23 0. https://linkinghub.elsevier.com/retrieve/pii/S0140700722002523. doi: 10.1016/j.ijrefrig.2022.07.004.
[16] Prouvé T, Charles I, Leenders H, et al. Progress on 30K-50K two Stage EM PT Cold Finger for Space Applications [J].
[17] Yang L. Investigation on a thermal-coupled two-stage Stirling-type pulse tube cryocooler[J]. Cryogenics, 2008, 4 8(11-12): 492-496. https://linkinghub.elsevier.com/retrieve/pii/S0011227508001094. doi: 10.1016/j.cryo genics.2008.07.003.
[18] Qiu L M, Zhi X Q, Han L, et al. Performance improvement of multi-stage pulse tube cryocoolers with a self-precoo led pulse tube[J]. Cryogenics, 2012, 52(10): 575-579. https://linkinghub.elsevier.com/retrieve/pii/S001122 751200094X. doi: 10.1016/j.cryogenics.2012.05.002.
[19] Xiaomin P, Xiaotao W, Wei D, et al. Numerical Study of a 10 K Two Stage Pulse Tube Cryocooler with Precooling I nside the Pulse Tube[J]. IOP Conference Series: Materials Science and Engineering, 2017, 171: 012071. https: //iopscience.iop.org/article/10.1088/1757-899X/171/1/012071. doi: 10.1088/1757-899X/171/1/01207 1.